Title: A New Perspective on Hydrogen Electrochemistry through Laviron–Amatore Paradox: Beyond Century-Long Paradigm

Author Names: Niraja Kurapati,[†] Rafael Martos Buoro,[†,‡] and Shigeru Amemiya[†,*,z]

Affiliation(s): [†]Department of Chemistry, University of Pittsburgh, 219 Parkman Avenue, Pittsburgh, Pennsylvania, 15260, United States. [‡]Instituto de Química de São Carlos, Universidade de São Paulo, 13566-590, São Carlos, SP, Brazil

[*]Electrochemical Society Member

[z]Corresponding Author E-mail Address [amemiya@pitt.edu]

Abstract

Herein, we advance our fundamental understanding of hydrogen electrochemistry as crucial energy technology by challenging the century-long paradigm that Volmer, Heyrovsky, and Tafel reactions are elementary. We identify and resolve the theoretical controversy of this phenomenological model to argue that each reaction must be stepwise not concerted elementarily. The stepwise model provides unprecedented insights as exemplified by resolving current debates on the Tafel analysis and volcano plot based on the controversial concerted model. The stepwise mechanism has not been distinguished from the concerted mechanism experimentally owing to the Laviron–Amatore paradox, which will be overcome by developing transient nanoelectrochemical methods.

Introduction

A greater understanding of hydrogen evolution reaction (*her*) and hydrogen oxidation reaction (*hor*) is urgently demanded both fundamentally (1) and practically (2) because these electrode reactions play crucial roles in electrochemical energy generation and storage. The renewed interest in these classical reactions is driven toward the development of new electrodes that are similarly reactive but less expensive than platinum, which tops the volcano plot (3). This challenging task has been addressed by designing and discovering earth-abundant electrocatalytic materials as guided by theory (4). The mechanism of *her* and *hor*, however, is far more complicated than represented by the forward and reverse directions of half-reaction, respectively

$$2H^+ + 2e^- \rightleftharpoons H_2 \quad (1)$$

where H^+ represents a proton donor, e.g., hydronium. Moreover, advanced electrochemical methods are required to measure the high *her* and *hor* activity of platinum (5, 6) and resolve bifurcated reaction pathways (7-9). The kinetic measurements were made with the acidic media, where *her* and *hor* are much faster than with the alkaline media (10, 11) to rationalize the minimal platinum required for the fuel cell anode (12) and enable the study of *her* at single platinum atoms (13).

Herein, we introduce the Laviron–Amatore paradox (14-16) to advance our fundamental understanding of hydrogen electrochemistry beyond the century-long paradigm that Volmer (17), Heyrovsky (18), and Tafel (19) reactions are elementary (20, 21). This traditional model divides *her* and *hor* (eq 1) into the respective reactions given by

$$M + H^+ + e^- \rightleftharpoons M - H \quad (2)$$

$$M - H + H^+ + e^- \rightleftharpoons H_2 + M \quad (3)$$

$$2M - H \rightleftharpoons H_2 + 2M \quad (4)$$

where M is an adsorption site on the electrode surface. We argue that none of these reactions can be concerted elementarily (Figure 1A), where the long-distance tunneling of proton and hydrogen is prohibited quantum-mechanically (22, 23) in contrast to long-distance electron

tunneling (24). We propose a new stepwise model (Figure 1B) as the inclusive alternative based on the Laviron–Amatore paradox not only to reinterpret the successful description of experimental *her* and *hor* kinetics by the phenomenological concerted model (7-9) but also to gain unprecedented insights into the mechanism of *her* and *hor* as exemplified by resolving current debates on the Tafel analysis (25) and volcano plot (26) based on the controversial concerted model. We urge that the paradox must be recognized and overcome to experimentally distinguish between concerted and stepwise mechanisms, which will be enabled by developing transient nanoelectrochemical methods based on ultrafast voltammetry (27) and scanning electrochemical microscopy (SECM) (28, 29).

Current Status

The concerted model based on elementary Volmer, Heyrovsky, and Tafel reactions has been exclusively accepted for a century (20, 21) to seriously limit our fundamental understanding of hydrogen electrochemistry as represented by current debates on the Tafel analysis (25) and the volcano plot (26). The concerted model was employed not only to predict theoretical volcano plots originally (30, 31) but also to debate the validity of volcano plot recently (26). Moreover, the free energy of hydrogen adsorption, ΔG_{H^*}, was calculated by density functional theory (DFT) to find the limited agreement between experimental and theoretical volcano plots (black circles and dashed line, respectively, in Figure 1C) (32), where the exchange current density, j^0, was underestimated experimentally (26) in comparison with the results of advanced measurements (7-9) (red symbols) and also misevaluated theoretically by using the concerted model erroneously (33, 34). Furthermore, the concerted model does not resolve the current debate on the origin of Butler–Volmer formula in the Tafel analysis (25). The Butler–Volmer formula can be only deduced from the concerted model for irreversible *her* or *hor* (35) to predict the dependence of Tafel slope on the rate-determining step and the hydrogen surface coverage (36). The same prediction was made recently by using the same concerted model (21), which was

called a microkinetic model (37), to demonstrate that the quasi-reversible kinetics based on both *her* and *hor* only "resembles" the Butler–Volmer formula.

We argue that each of Volmer, Heyrovsky, and Tafel reactions must be mediated through the stepwise mechanism (Figure 1B) instead of the concerted mechanism (Figure 1A), where the long-distance tunneling of proton and hydrogen is quantum-mechanically prohibited (22, 23). In the concerted Vomer reaction, the electrodeposition of hydrogen at the inner Helmholtz plane requires proton tunneling from the outer Helmholtz plane, which far exceeds possible tunneling distances of ~1 Å (22, 23). Accordingly, the proton donor must be pre-adsorbed at the inner-Helmholtz plane to electrodeposit hydrogen on the electrode surface in a single step, thereby requiring the stepwise mechanism (38). Similarly, the Heyrovsky reaction must be initiated by the specific adsorption of proton donor (39), which avoids the long-distance tunneling of hydrogen in contrast to the concerted mechanism. Subsequently, the stepwise Heyrovsky reaction shares the adsorption of dihydrogen with the Tafel reaction, which must be also stepwise owing to the preceding formation of adsorbed dihydrogen. By contrast, the coupling between Heyrovsky and Tafel reactions is not obvious in the concerted model and has not been recognized. Moreover, the hydronium adsorbed on Au and Pt electrodes was detected spectroscopically (40, 41) to draw no attention as a possible intermediate, the lack of which is required for an elementary chemical reaction (42). These examples represent the unconscious and unchallenged acceptance of the concerted mechanism.

We also argue that the Butler–Volmer formula of elementary electron transfer is fundamentally incompatible with the concerted model because Volmer and Heyrovsky reactions are not elementary. The single transition state required for an elementary chemical reaction (42) is represented by the single standard rate constant at the formal potential in the Butler–Volmer formula (43). By contrast, the rate of concerted Volmer reaction, v_{V}, is given by two rate constants, k_1^0 and k_{-1}^0, at the formal potential, E_1^0, as (44)

$$v_{\mathrm{V}} = k_1^0 \Gamma_{\mathrm{s}} [\mathrm{H}^+](1-\theta_{\mathrm{H}}) \exp[-\alpha f(E-E_1^0)] - k_{-1}^0 \Gamma_{\mathrm{s}} \theta_{\mathrm{H}} \exp[(1-\alpha) f(E-E_1^0)] \quad (5)$$

where Γ_s is the saturated surface concentration of adsorbate and is dependent on the concentration of electrode surface atom and the number of adsorbates on each surface atom (45), $[H^+]$ is the concentration of proton donor near the electrode surface, θ_H is the fraction of adsorbed hydrogen, $f = RT/F$, α is the transfer coefficient, and E is the electrode potential. The same symbol, α, is employed to represent the transfer coefficient of all relevant reactions for simplicity. The rate of concerted Heyrovsky reaction, v_H, is defined also by two rate constants, k_2^0 and k_{-2}^0, at the formal potential, E_2^0, to yield (44)

$$v_H = k_2^0 \Gamma_s \theta_H [H^+] \exp[-\alpha f(E - E_2^0)] - k_{-2}^0 \Gamma_s (1 - \theta_H)[H_2] \exp[(1 - \alpha) f(E - E_2^0)] \quad (6)$$

where $[H_2]$ is the concentration of dihydrogen near the electrode surface. The concerted model also gives the potential-independent rate of non-electrochemical Tafel reaction, v_T, as (44)

$$v_T = k_3^0 (\Gamma_s \theta_H)^2 - k_{-3}^0 [\Gamma_s (1 - \theta_H)]^2 [H_2] \quad (7)$$

where k_3^0 and k_{-3}^0 are forward and reverse rate constants, respectively.

Despite the theoretical controversy, the concerted model agrees with the experimental kinetics of Volmer, Heyrovsky, and Tafel reactions quantitatively (7-9), which we attribute to the Laviron–Amatore paradox. While this terminology was introduced only recently by us (14, 15) and referred to by Amatore (16), Laviron (46) and Amatore (47) established much earlier that the outer-sphere electron transfer of non-adsorbed redox couple at the outer Helmholtz plane can not be distinguished electrochemically from the inner-sphere electron transfer of adsorbed form at the inner Helmholtz plane when adsorption equilibria are maintained. More relevantly, Amatore and co-workers extended the paradox to the Volmer-type reaction based on inner-sphere electron transfer to predict that the concerted mechanism is equivalent to the stepwise mechanism electrochemically when the equilibrium adsorption of reactant is maintained (48). The paradox, however, has not been extended to the Heyrovsky reaction or the Volmer reaction based on proton-coupled inner-sphere electron transfer.

Future Needs and Prospects

The century-old concerted model based on elementary Volmer, Heyrovsky, and Tafel reactions is phenomenological and controversial, which must be recognized and resolved to advance our fundamental understanding of hydrogen electrochemistry. We attribute the controversy to the Laviron–Amatore paradox (14-16), which is proved by modeling stepwise Volmer, Heyrovsky, and Tafel reactions for the first time and comparing the stepwise model with the concerted model. Either model is based on both *her* and *hor* and applicable to diffusional mass transport under any electrochemical measurement. The stepwise model must be confirmed experimentally by overcoming the paradox, which will be enabled by transient nanoelectrochemical methods.

Stepwise Model. We propose the stepwise model based on the equilibrium adsorption of proton donner and dihydrogen as required for the Laviron–Amatore paradox to manifest proton-coupled inner-sphere electron transfer (red arrows in Figure 1B) as the elementary rate-determining steps of Volmer and Heyrovsky reactions. The corresponding kinetics is described by the Butler–Volmer formula of elementary electron transfer as confirmed experimentally (see below). Specifically, proton-coupled inner-sphere electron transfer in the stepwise Volmer reaction is given by

$$\mathrm{M\cdots H^+ + e^- \rightleftharpoons M-H} \tag{8}$$

with

$$v_\mathrm{V} = k_\mathrm{V}^0\Gamma_\mathrm{s}\theta_{\mathrm{H^+}}\exp[-\alpha f(E-E_\mathrm{V}^0)] - k_\mathrm{V}^0\Gamma_\mathrm{s}\theta_\mathrm{H}\exp[(1-\alpha)f(E-E_\mathrm{V}^0)] \tag{9}$$

where k_V^0 and E_V^0 are a standard rate constant and a formal potential, respectively. The stepwise Heyrovsky reaction involves

$$\mathrm{M-H\cdots H^+ + e^- \rightleftharpoons M\cdots H_2} \tag{10}$$

with

$$v_\mathrm{H} = k_\mathrm{H}^0\Gamma_\mathrm{s}\theta_{\mathrm{HH^+}}\exp[-\alpha f(E-E_\mathrm{H}^0)] - k_\mathrm{H}^0\Gamma_\mathrm{s}\theta_{\mathrm{H_2}}\exp[(1-\alpha)f(E-E_\mathrm{H}^0)] \tag{11}$$

where k_H^0 and E_H^0 are a standard rate constant and a formal potential, respectively.

In the stepwise model, equilibrium adsorption is described by the Langmuir isotherm for

simplicity. The adsorption of proton donor in the stepwise Volmer reaction is given by

$$\mathrm{M} + \mathrm{H}^+ \rightleftharpoons \mathrm{M} \cdots \mathrm{H}^+ \tag{12}$$

with

$$\beta_{\mathrm{H}^+}[\mathrm{H}^+] = \frac{\theta_{\mathrm{H}^+}}{\theta_{\mathrm{M}}} \tag{13}$$

where β_{H^+} is the equilibrium constant, and θ_{H^+} and θ_{M} are fractions of adsorbed proton donor and free adsorption site, respectively. The stepwise Heyrovsky reaction involves the adsorption of proton donor

$$\mathrm{M} - \mathrm{H} + \mathrm{H}^+ \rightleftharpoons \mathrm{M} - \mathrm{H} \cdots \mathrm{H}^+ \tag{14}$$

with

$$\beta_{\mathrm{HH}^+}[\mathrm{H}^+] = \frac{\theta_{\mathrm{HH}^+}}{\theta_{\mathrm{H}}} \tag{15}$$

and the adsorption of dihydrogen

$$\mathrm{M} + \mathrm{H}_2 \rightleftharpoons \mathrm{M} \cdots \mathrm{H}_2 \tag{16}$$

with

$$\beta_{\mathrm{H}_2}[\mathrm{H}_2] = \frac{\theta_{\mathrm{H}_2}}{\theta_{\mathrm{M}}} \tag{17}$$

where β_{HH^+} and β_{H_2} are the corresponding equilibrium constants, θ_{HH^+} is the fraction of proton donor on the adsorbed hydrogen, and θ_{H_2} is the fraction of adsorbed dihydrogen.

Finally, the stepwise Tafel reaction includes the equilibrium adsorption of dihydrogen (eq 16) and the formation of adsorbed dihydrogen at the electrode surface as given by

$$2\mathrm{M} - \mathrm{H} \rightleftharpoons \mathrm{M} \cdots \mathrm{H}_2 + \mathrm{M} \tag{18}$$

with

$$v_{\mathrm{T}} = k_{+\mathrm{T}}(\Gamma_{\mathrm{s}}\theta_{\mathrm{H}})^2 - k_{-\mathrm{T}}(\Gamma_{\mathrm{s}})^2\theta_{\mathrm{H}_2}\theta_{\mathrm{M}} \tag{19}$$

where v_{T} is the corresponding rate, and $k_{+\mathrm{T}}$ and $k_{-\mathrm{T}}$ are association and dissociation rate constants, respectively.

Laviron–Amatore Paradox. We prove the Laviron–Amatore paradox for *her* and *hor* by demonstrating that each of concerted Volmer, Heyrovsky, and Tafel reactions is electrochemically equivalent to the stepwise counterpart when the equilibrium adsorption of

proton donor and dihydrogen is maintained. This proof requires the dominance of hydrogen on the electrode surface, i.e., $\theta_{\mathrm{H}} >> \theta_{\mathrm{H}^+}$, θ_{HH^+}, and θ_{H_2}, to yield

$$\theta_{\mathrm{H}} + \theta_{\mathrm{M}} = 1 \tag{20}$$

For comparisons, the rates of Volmer and Heyrovsky reactions are defined against the overpotential, η (= $E - E^*$), where E^* is an equilibrium potential and is equivalent to the potential of reference electrode experimentally. The rates of stepwise reactions were derived similarly as reported for the concerted counterparts (44).

The paradox is proved for concerted and stepwise Volmer reactions by the common form of reaction rate, i.e.,

$$v_{\mathrm{V}} = v_1^0 \left\{ \left(\frac{[\mathrm{H}^+]}{[\mathrm{H}^+]^*} \right) \left(\frac{1-\theta_{\mathrm{H}}}{1-\theta_{\mathrm{H}}^*} \right) \exp(-\alpha f \eta) - \left(\frac{\theta_{\mathrm{H}}}{\theta_{\mathrm{H}}^*} \right) \exp[(1-\alpha) f \eta] \right\} \tag{21}$$

where v_1^0 is the rate of forward and reverse reactions at $\eta = 0$, and θ_{H}^* and $[\mathrm{H}^+]^*$ are the fraction of adsorbed hydrogen atoms and the bulk concentration of proton donor at the equilibrium condition, respectively. The equilibrium rate is given for the respective reactions by

$$v_1^0 = {k_1^0}^{(1-\alpha)} {k_{-1}^0}^{\alpha} \Gamma_{\mathrm{s}} [\mathrm{H}^+]^{*(1-\alpha)} (\theta_{\mathrm{H}}^*)^{\alpha} (1-\theta_{\mathrm{H}}^*)^{(1-\alpha)} \tag{22}$$

$$v_1^0 = k_{\mathrm{V}}^0 {\beta_{\mathrm{H}^+}}^{(1-\alpha)} \Gamma_{\mathrm{s}} [\mathrm{H}^+]^{*(1-\alpha)} (\theta_{\mathrm{H}}^*)^{\alpha} (1-\theta_{\mathrm{H}}^*)^{(1-\alpha)} \tag{23}$$

Eqs 22 and 23 are equivalent to each other with

$${k_1^0}^{(1-\alpha)} {k_{-1}^0}^{\alpha} = k_{\mathrm{V}}^0 {\beta_{\mathrm{H}^+}}^{(1-\alpha)} \tag{24}$$

Since α is potential-dependent in theory (24), eq 24 is satisfied at any equilibrium potential with

$$k_1^0 = k_{\mathrm{V}}^0 \beta_{\mathrm{H}^+} \tag{25}$$

$$k_{-1}^0 = k_{\mathrm{V}}^0 \tag{26}$$

Eq 25 confirms that the proton-coupled inner-sphere reduction of adsorbed proton donor is preceded by the equilibrium adsorption of proton donor in the stepwise Volmer reaction to yield the convoluted forward rate constant for the concerted Volmer reaction, thereby deviating from the Butler–Volmer formula. By contrast, eq 26 indicates that the reverse direction of both concerted and stepwise Volmer reactions represents the elementary proton-coupled inner-sphere oxidation of adsorbed hydrogen to follow the formula.

The rates of concerted and stepwise Heyrovsky reactions are given also by a common form with an equilibrium rate constant, v_2^0, as

$$v_{\mathrm{H}} = v_2^0 \left\{ \left(\frac{[\mathrm{H}^+]}{[\mathrm{H}^+]^*} \right) \left(\frac{\theta_{\mathrm{H}}}{\theta_{\mathrm{H}}^*} \right) \exp(-\alpha f \eta) - \left(\frac{[\mathrm{H}_2]}{[\mathrm{H}_2]^*} \right) \left(\frac{1-\theta_{\mathrm{H}}}{1-\theta_{\mathrm{H}}^*} \right) \exp[(1-\alpha) f \eta] \right\} \tag{27}$$

where $[\mathrm{H}_2]^*$ is the bulk concentration of dihydrogen at the equilibrium condition. The respective mechanisms yield

$$v_2^0 = {k_2^0}^{(1-\alpha)} {k_{-2}^0}^{\alpha} \Gamma_{\mathrm{s}} [\mathrm{H}^+]^{*(1-\alpha)} [\mathrm{H}_2]^{*\alpha} (\theta_{\mathrm{H}}^*)^{(1-\alpha)} (1-\theta_{\mathrm{H}}^*)^{\alpha} \tag{28}$$

$$v_2^0 = {k_{\mathrm{H}}^0 \beta_{\mathrm{HH}^+}}^{(1-\alpha)} {\beta_{\mathrm{H}_2}}^{\alpha} \Gamma_{\mathrm{s}} [\mathrm{H}^+]^{*(1-\alpha)} [\mathrm{H}_2]^{*\alpha} (\theta_{\mathrm{H}}^*)^{(1-\alpha)} (1-\theta_{\mathrm{H}}^*)^{\alpha} \tag{29}$$

Eqs 28 and 29 are equivalent to each other with

$${k_2^0}^{(1-\alpha)} {k_{-2}^0}^{\alpha} = {k_{\mathrm{H}}^0 \beta_{\mathrm{HH}^+}}^{(1-\alpha)} {\beta_{\mathrm{H}_2}}^{\alpha} \tag{30}$$

The equivalence of α-independent portions of eq 30 requires

$$k_2^0 = k_{\mathrm{H}}^0 \beta_{\mathrm{HH}^+} \tag{31}$$

A combination of eq 30 with eq 31 gives

$$k_{-2}^0 = k_{\mathrm{H}}^0 \beta_{\mathrm{H}_2} \tag{32}$$

Eqs 31 and 32 indicate that the equilibrium adsorption of proton donor and dihydrogen precedes proton-coupled inner-sphere reduction and oxidation, respectively, in the Heyrovsky reaction, which deviates from the Butler–Volmer formula in the concerted mechanism.

Finally, the kinetics of concerted and stepwise Tafel reactions is described equally by

$$v_{\mathrm{T}} = v_3^0 \left\{ \left(\frac{\theta_{\mathrm{H}}}{\theta_{\mathrm{H}}^*} \right)^2 - \left(\frac{1-\theta_{\mathrm{H}}}{1-\theta_{\mathrm{H}}^*} \right)^2 \left(\frac{[\mathrm{H}_2]}{[\mathrm{H}_2]^*} \right) \right\} \tag{33}$$

where v_3^0 (mol/cm^2/s) is a rate constant at the equilibrium condition and is given by

$$v_3^0 = k_3^0 (\Gamma_{\mathrm{s}} \theta_{\mathrm{H}}^*)^2 = k_{+\mathrm{T}} (\Gamma_{\mathrm{s}} \theta_{\mathrm{H}}^*)^2 \tag{34}$$

to find

$$k_3^0 = k_{+\mathrm{T}} \tag{35}$$

Also, we assessed the thermodynamics of concerted and stepwise Tafel reactions to yield

$$k_{-3}^0 = k_{-\mathrm{T}} \beta_{\mathrm{H}_2} \tag{36}$$

Importantly, β_{H_2} is included in the rate constants of both Heyrovsky and Tafel reactions (eqs 32

and 36, respectively), which share the equilibrium adsorption of dihydrogen. The common pathway is obvious in the stepwise mechanism but not in the concerted mechanism.

Tafel Analysis. The stepwise model is supported experimentally to reveal that the Butler–Volmer formula in the Tafel analysis originates from proton-coupled inner-sphere electron transfer, which is unconsidered in the concerted model (21, 35, 36) to cause the current debate on the origin (25). The Butler–Volmer formula of proton-coupled inner-sphere electron transfer (eqs 9 and 11) was ensured by quasi-reversible voltammograms of *her* and *hor* in the acidic aqueous media (7-9), which agreed well with the concerted model (eqs 21, 27, and 33) as the equivalent of the stepwise model owing to the Laviron–Amatore paradox. In these advanced experiments, voltammetric responses based on bifurcated Volmer–Heyrovsky and Volmer–Tafel pathways were resolved under high mass-transport conditions of nanoelectrodes (7) or SECM (8, 9) not only to separately determine v_1^0, v_2^0, and v_3^0 but also to obtain the transfer coefficient of 0.5 for proton-coupled inner-sphere electron transfer in Volmer and Heyrovsky reactions by modeling the potential-dependence of hydrogen surface coverage, θ_{H}. This result rationalizes the use of the Marcusian transfer coefficient in the Tafel analysis of irreversible *her* or *hor* (21, 35, 36).

Moreover, the stepwise model is compatible with the anomalous Tafel slopes reported recently for *her* of triethylammonium and diisopropylethylammonium as proton donors at the Au electrode in acetonitrile (49). Quantum theory attributed the corresponding non-Marcusian transfer coefficients to the non-adiabaticity of proton-coupled inner-sphere electron transfer in the Volmer reaction (50), which is implemented in the stepwise model but not in the concerted model.

Volcano Plot. We apply the stepwise model to gain new insights into volcano plots, which were proposed (30, 31) and have been debated (26) by using the concerted model exclusively. We employ the stepwise model to obtain the theoretical volcano plot of the exchange current density, j^0, against the free energy of hydrogen adsorption, ΔG_{H^*}. The current density, j, based on *her* and *hor* is given by the Faraday's law for electrochemical Volmer and Heyrovsky reactions as (7)

$$j = F(v_{\mathrm{V}} + v_{\mathrm{H}}) \tag{37}$$

The exchange current density is obtained from either anodic or cathodic components of eq 37 at $\eta = 0$, where $\theta_{\mathrm{H}} = \theta_{\mathrm{H}}^*$, $[\mathrm{H}^+] = [\mathrm{H}^+]^*$, and $[\mathrm{H}_2] = [\mathrm{H}_2]^*$ in eqs 21 or 27 result in

$$j^0 = F(v_1^0 + v_2^0) \tag{38}$$

Both concerted and stepwise models give the common form of exchange current density by combining eq 38 with eqs 22 and 28 and with eqs 23 and 29, respectively, where $\alpha = 0.5$ yields

$$j^0 = (f_{\mathrm{V}} + f_{\mathrm{H}})\sqrt{\theta_{\mathrm{H}}^*(1 - \theta_{\mathrm{H}}^*)} \tag{39}$$

with

$$f_{\mathrm{V}} = \Gamma_{\mathrm{s}}\sqrt{k_1^0 k_{-1}^0 [\mathrm{H}^+]^*} = \Gamma_{\mathrm{s}} k_{\mathrm{V}}^0 \sqrt{\beta_{\mathrm{H}^+}[\mathrm{H}^+]^*} \tag{40}$$

$$f_{\mathrm{H}} = \Gamma_{\mathrm{s}}\sqrt{k_2^0 k_{-2}^0 [\mathrm{H}^+]^*[\mathrm{H}_2]^*} = \Gamma_{\mathrm{s}} k_{\mathrm{H}}^0 \sqrt{\beta_{\mathrm{HH}^+}\beta_{\mathrm{H}_2}[\mathrm{H}^+]^*[\mathrm{H}_2]^*} \tag{41}$$

Also, we define ΔG_{H^*} for the adsorption of one hydrogen atom based on the Tafel reaction (not two as defined by eqs 4 and 18) to yield

$$\exp\left(-\frac{\Delta G_{\mathrm{H}^*}}{RT}\right) = \frac{\theta_{\mathrm{H}}^*}{1-\theta_{\mathrm{H}}^*} = \sqrt{\frac{[\mathrm{H}_2]^*}{K_3}} = \sqrt{\frac{\beta_{\mathrm{H}_2}[\mathrm{H}_2]^*}{K_{\mathrm{T}}}} \tag{42}$$

where K_3 $(= k_3^0/k_{-3}^0)$ and K_{T} $(= k_{+\mathrm{T}}/k_{-\mathrm{T}})$ are equilibrium constants. Eq 42 is used to calculate the $\sqrt{\theta_{\mathrm{H}}^*(1 - \theta_{\mathrm{H}}^*)}$ term of eq 39 against ΔG_{H^*}.

We consider the coupling between Heyrovsky and Tafel reactions to predict the theoretical volcano plot based on the stepwise model. This coupling was unidentified in the concerted model to make the invalid assumption that only θ_{H}^* varies with ΔG_{H^*} to yield a volcano plot while f_{V} and f_{H} are independent of ΔG_{H^*} (30, 31). By contrast, the stepwise model indicates that f_{H} can also vary with ΔG_{H^*} because both f_{H} (eq 41) and ΔG_{H^*} (eq 42) include β_{H_2} for the common pathway of dihydrogen adsorption between Heyrovsky and Tafel reactions (Figure 1B). The coupling can be neglected to obtain a volcano plot only if the Volmer reaction dominates the exchange current density as demonstrated below, i.e., $j^0 \approx F v_1^0$ from eq 38 with $v_1^0 \gg v_2^0$, or if the electrode-dependence of ΔG_{H^*} is caused not by β_{H_2} but by K_{T}, which is not included in f_{V} or f_{H}.

The theoretical volcano plot based on the stepwise model (eq 39) agrees well with

experimental and theoretical data in the literature to account for the superior *her* and *hor* activity of platinum in the acidic aqueous media. We calculated experimental exchange current densities at Pt and Au electrodes from eq 38 with the v_1^0 and v_2^0 values determined separately by voltammetry with nanoelectrodes (7) or SECM (8, 9) as discussed above. The conditional v_1^0 and v_2^0 values against reversible hydrogen electrodes were corrected against the normal hydrogen electrode (51). The resultant exchange current density at Pt nanoelectrodes (red circle in Figure 1C) is consistent with that of Pt SECM tips (red cross) but is somehow higher than that at the macroscopic Pt substrates of SECM (red triangle), where mass transport was efficient enough to determine v_1^0 and v_2^0 separately. We plotted experimental and theoretical exchange current densities against ΔG_{H^*} as estimated by DFT for various metals in a vacuum (32). The exchange current densities based on eq 39 (red solid line) agreed well with those at Pt nanoelectrodes and Pt and Au (red square) SECM tips, where $v_1^0 \gg v_2^0$ resulted in $f_{\mathrm{V}} + f_{\mathrm{H}} \approx f_{\mathrm{V}}$ = 36 A/cm^2 in addition to a transfer coefficient of 0.5 as ensured separately by the slope of the plot. The experimental v_2^0 values are negligibly small owing to the low equilibrium concentration of dihydrogen (see eq 29), e.g., $[\mathrm{H_2}]^* = 5.9 \times 10^{-7}$ mol/cm^3 in 0.5 M H_2SO_4 at 1 atm (52). Since the adsorption of hydronium on Pt and Au electrodes is similarly weak (40, 41), similar f_{V} values of ~36 A/cm^2 at these electrodes correspond to the negligible metal-dependence of k_{V}^0 (see eq 40), which indicates that proton-coupled inner-sphere electron transfer in the Volmer reaction is adiabatic, i.e., solvent-controlled (23). Accordingly, the exchange current density in the acidic media is highest with platinum, which yields $\theta_{\mathrm{H}}^* \approx 0.5$ to maximize $\sqrt{\theta_{\mathrm{H}}^*(1-\theta_{\mathrm{H}}^*)}$ in eq 39.

The theoretical volcano plot based on the stepwise model (eq 39) integrates experimental exchange current densities and DFT-based ΔG_{H^*} to resolve the current debate on the validity of volcano plot (26). By contrast, the original theoretical plot against DFT-based ΔG_{H^*} employed the concreted model (black dashed line in Figure 1C) to only partially agree with experimental exchange current densities at macroscopic electrodes (black circles) (32). We found that the original plot is steeper than expected from the equivalent stepwise model (red solid line) to

confirm the erroneous use of the concerted model as pointed out by Schmickler and Trasatti (33) and admitted by Nørskov (34). A similarly steep plot was reported later by calculating the DFT-based exchange current density solely from the rate of the non-electrochemical Tafel reaction (53), which contradicts the Faraday's law (7). Moreover, the experimental exchange current densities at macroscopic electrodes were underestimated owing to low mass-transport conditions (11) to lower the original plot against DFT-based ΔG_{H^*} and also yield a low $f_V + f_H$ value of 6.6 mA/cm^2 from a better fit with the stepwise model (black solid line). The similarly low peak of Trasatti's experimental plot around 3 mA/cm^2 (3) indicates that the establishment of experimental volcano plot requires reliable v_1^0 and v_2^0 values at various electrodes.

Overcoming the Paradox. Finally, we propose nanoscale transient voltammetry as a powerful approach to overcome the paradox for *her* and *hor* as well as other adsorption-coupled electron-transfer reactions (14), which are important in electrocatalysis and electrodeposition. Theoretically, Amatore and co-workers modeled transient voltammetry of Volmer-type reaction to predict that concerted and stepwise mechanisms are distinguishable when the adsorption of reactant is sufficiently slow and weak (48). The respective conditions are given for the Volmer reaction by

$$k_{H^+}^{ads}[H^+]^* \frac{f}{v} \ll 1 \quad (43)$$

$$\beta_{MH^+}[H^+]^* \ll 1 \quad (44)$$

where $k_{H^+}^{ads}$ is the rate constant for the adsorption of proton donor and *v* is the potential scan rate. Eqs 43 and 44 imply that the transient desorption of proton donor from the electrode surface is controlled kinetically and detected sensitively at sufficiently fast scan rates to prove the stepwise mechanism (48), which is facilitated by employing a lower concentration of proton donor in solution to favor both conditions.

Experimentally, the paradox was overcome by microscale transient voltammetry to resolve outer-sphere and inner-sphere electron transfer in electrocatalysis and electrodeposition. Ultrafast voltammetry at scan rates of up to 10 kV/s revealed the inner-sphere reduction of benzyl chloride at the silver microelectrode (54). SECM-based transient voltammetry with sub-micrometer tip–

substrate gaps resolved the electrodeposition of magnetite into outer-sphere electron transfer and the following surface reaction of an intermediate adsorbate (55), which was otherwise undetectable electrochemically and spectroscopically.

We envision that ultrafast voltammetry and SECM-based voltammetry are reinforced at the nanoscale to experimentally reveal the true mechanisms of Volmer, Heyrovsky, and Tafel reactions and beyond. Advantageously, a pair of electrodes with a nanometer-wide gap facilitates quantitative ultrafast voltammetry by monitoring the product of voltammetric generator electrode at the amperometric collector electrode (56), where the capacitive background current is largely suppressed (57). The kinetic resolution of SECM-based voltammetry is enhanced by employing a nanometer tip–substrate gap, which requires faster potential sweep to obtain transient responses to redox-active adsorbates (58).

Conclusions

We identified and resolved the century-long controversy of elementary Volmer, Heyrovsky, and Tafel reactions to advance our fundamental understanding of hydrogen electrochemistry. We proposed a stepwise model not only to prove the attribution of the currently unrecognized controversy to the Laviron–Amatore paradox but also to resolve current debates on the Tafel analysis and the volcano plot. The stepwise model revealed proton-coupled inner-sphere electron transfer as the elementary rate-determining steps of Volmer and Heyrovsky reactions. Subsequently, the stepwise model is compatible with the Butler–Volmer formula of elementary electron transfer to implement the experimental Tafel slopes based on either Marcusian or non-Marcusian transfer coefficients. Moreover, the coupling between Heyrovsky and Tafel reactions was identified by the stepwise model to establish a theoretical volcano plot by integrating experimental and theoretical data. This agreement implies that the highest *her* and *hor* activity of platinum in the acidic aqueous media represents the solvent-control of proton-coupled inner-sphere electron transfer in the Volmer reaction. We envision that the paradox can be overcome experimentally by nanoscale transient voltammetry in future work to manifest the true

mechanisms of *her*, *hor*, and beyond.

Acknowledgments

This work was supported by the National Science Foundation (CHE-1904258) and São Paulo Foundation Research (Grant 2019/06621-3).

References

1. A. J. Bard, *J. Am. Chem. Soc.*, **132**, 7559 (2010).
2. M. K. Debe, *Nature*, **486**, 43 (2012).
3. S. Trasatti, *J. Electroanal. Chem. Interfacial Electrochem.*, **39**, 163 (1972).
4. Z. W. Seh, J. Kibsgaard, C. F. Dickens, I. B. Chorkendorff, J. K. Nørskov and T. F. Jaramillo, *Science*, **355** (2017).
5. J. Zhou, Y. Zu and A. J. Bard, *J. Electroanal. Chem.*, **491**, 22 (2000).
6. S. Chen and A. Kucernak, *J. Phys. Chem. B*, **108**, 13984 (2004).
7. J. X. Wang, T. E. Springer and R. R. Adzic, *J. Electrochem. Soc.*, **153**, A1732 (2006).
8. H. L. Bonazza, L. D. Vega and J. L. Fernández, *J. Electroanal. Chem.*, **713**, 9 (2014).
9. M. A. B. Helu and J. L. Fernández, *J. Electroanal. Chem.*, **784**, 33 (2017).
10. J. H. Barber and B. E. Conway, *J. Electroanal. Chem.*, **461**, 80 (1999).
11. W. Sheng, H. A. Gasteiger and Y. Shao-Horn, *J. Electrochem. Soc.*, **157**, B1529 (2010).
12. J. Durst, C. Simon, F. Hasche and H. A. Gasteiger, *J. Electrochem. Soc.*, **162**, F190 (2015).
13. M. Zhou, J. E. Dick and A. J. Bard, *J. Am. Chem. Soc.*, **139**, 17677 (2017)

14. S. Amemiya, Nanoelectrochemistry of Adsorption-Coupled Electron Transfer at Carbon Electrodes in *Nanocarbon Electrochemistry*, N. Yang, G. Zhao and J. Foord Editors, p. 1, John Wiley & Sons, New York (2020).

15. N. Kurapati, P. Pathirathna, C. J. Ziegler and S. Amemiya, *ChemElectroChem*, **6**, 5651 (2019).

16. A. Oleinick, I. Svir and C. Amatore, *J. Solid State Electrochem.* **24**, 2023 (2020).

17. T. Erdey-Grúz and M. Volmer, *Z. Phys. Chem.*, **150A**, 203 (1930).

18. J. Heyrovský, *Recl. Trav. Chim. Pays-Bas*, **46**, 582 (1927).

19. J. Tafel, *Z. Phys. Chem.*, **50U**, 641 (1905).

20. B. E. Conway and B. V. Tilak, *Electrochim. Acta*, **47**, 3571 (2002).

21. T. Shinagawa, A. T. Garcia-Esparza and K. Takanabe, *Sci. Rep.*, **5**, 13801 (2015).

22. Y. C. Lam, A. V. Soudackov, Z. K. Goldsmith and S. Hammes-Schiffer, *J. Phys. Chem. C*, **123**, 12335 (2019).

23. Y. C. Lam, A. V. Soudackov and S. Hammes-Schiffer, *J. Phys. Chem. Lett.*, **10**, 5312 (2019).

24. R. A. Marcus, *J. Chem. Phys.*, **43**, 679 (1965).

25. E. J. F. Dickinson and G. Hinds, *J. Electrochem. Soc.*, **166**, F221 (2019).

26. P. Quaino, F. Juarez, E. Santos and W. Schmickler, *Beilstein J. Nanotechnol.*, **5**, 846 (2014).

27. X. S. Zhou, B. W. Mao, C. Amatore, R. G. Compton, J. L. Marignier, M. Mostafavi, J. F. Nierengarten and E. Maisonhaute, *Chem. Commun.*, **52**, 251 (2016).

28. S. Amemiya, Nanoscale Scanning Electrochemical Microscopy in *Electroanalytical Chemistry*, A. J. Bard and C. G. Zoski Editors, p. 1, CRC Press, Boca Raton, FL (2015).

29. T. Kai, C. G. Zoski and A. J. Bard, *Chem. Commun.*, **54**, 1934 (2018).

30. R. Parsons, *Trans. Faraday Soc.*, **54**, 1053 (1958).

31. H. Gerischer, *Bull. Soc. Chim. Belg.*, **67**, 506 (1958).

32. J. K. Nørskov, T. Bligaard, A. Logadottir, J. R. Kitchin, J. G. Chen, S. Pandelov and U. Stimming, *J. Electrochem. Soc.*, **152**, J23 (2005).

33. W. Schmickler and S. Trasatti, *J. Electrochem. Soc.*, **153**, L31 (2006).

34. J. K. Nørskov, T. Bligaard, A. Logadottir, J. R. Kitchin, J. G. Chen, S. Pandelov and U. Stimming, *J. Electrochem. Soc.*, **153**, L33 (2006).

35. J. O. M. Bockris and H. Mauser, *Can. J. Chem.*, **37**, 475 (1959).

36. J. O. M. Bockris and D. F. A. Koch, *J. Phys. Chem.*, **65**, 1941 (1961).

37. A. H. Motagamwala, M. R. Ball and J. A. Dumesic, *Annu. Rev. Chem. Biomol. Eng.*, **9**, 413 (2018).

38. S. Fletcher, *J. Solid State Electrochem.*, **13**, 537 (2009).

39. E. Santos, P. Hindelang, P. Quaino and W. Schmickler, *Phys. Chem. Chem. Phys.*, **13**, 6992 (2011).

40. K. Ataka, T. Yotsuyanagi and M. Osawa, *J. Phys. Chem.*, **100**, 10664 (1996).

41. M. Osawa, M. Tsushima, H. Mogami, G. Samjeské and A. Yamakata, *J. Phys. Chem. C*, **112**, 4248 (2008).

42. K. J. Laidler, *Pure Appl. Chem.*, **68**, 149 (1996).

43. A. J. Bard and L. R. Faulkner, *Electrochemical Methods: Fundamentals and Applications*, p. 92, John Wiley & Sons, New York (2001).

44. A. Lasia, *Int. J. Hydrogen Energy*, **44**, 19484 (2019).

45. J. X. Wang, T. E. Springer, P. Liu, M. Shao and R. R. Adzic, *J. Phys. Chem. C*, **111**, 12425 (2007).

46. E. Laviron, *J. Electroanal. Chem.*, **382**, 111 (1995).

47. O. V. Klymenko, I. Svir and C. Amatore, *J. Electroanal. Chem.*, **688**, 320 (2013).

48. O. V. Klymenko, I. Svir and C. Amatore, *Mol. Phys.*, **112**, 1273 (2014).

49. M. N. Jackson and Y. Surendranath, *J. Am. Chem. Soc.*, **138**, 3228 (2016).

50. Z. K. Goldsmith, Y. C. Lam, A. V. Soudackov and S. Hammes-Schiffer, *J. Am. Chem. Soc.*,**141**, 1084 (2019).

51. G. Jerkiewicz, *ACS Catalysis*, **10**, 8409 (2020).

52. R. M. Q. Mello and E. A. Ticianelli, *Electrochim. Acta*, **42**, 1031 (1997).

53. E. Skúlason, V. Tripkovic, M. E. Björketun, S. Gudmundsdóttir, G. Karlberg, J. Rossmeisl, T. Bligaard, H. Jónsson and J. K. Nørskov, *J. Phys. Chem. C*, **114**, 18182 (2010).

54. O. V. Klymenko, O. Buriez, E. Labbe, D. P. Zhan, S. Rondinini, Z. Q. Tian, I. Svir and C. Amatore, *ChemElectroChem*, **1**, 227 (2014).

55. M. A. Bhat, N. Nioradze, J. Kim, S. Amemiya and A. J. Bard, *J. Am. Chem. Soc.*, **139**, 15891 (2017).

56. P. Pathirathna, R. J. Balla and S. Amemiya, *J. Electrochem. Soc.*, **165**, G3026 (2018).

57. P. Pathirathna, R. J. Balla and S. Amemiya, *Anal. Chem.*, **90**, 11746 (2018).

58. R. Chen, R. J. Balla, Z. T. Li, H. T. Liu and S. Amemiya, *Anal. Chem.*, **88**, 8323 (2016).

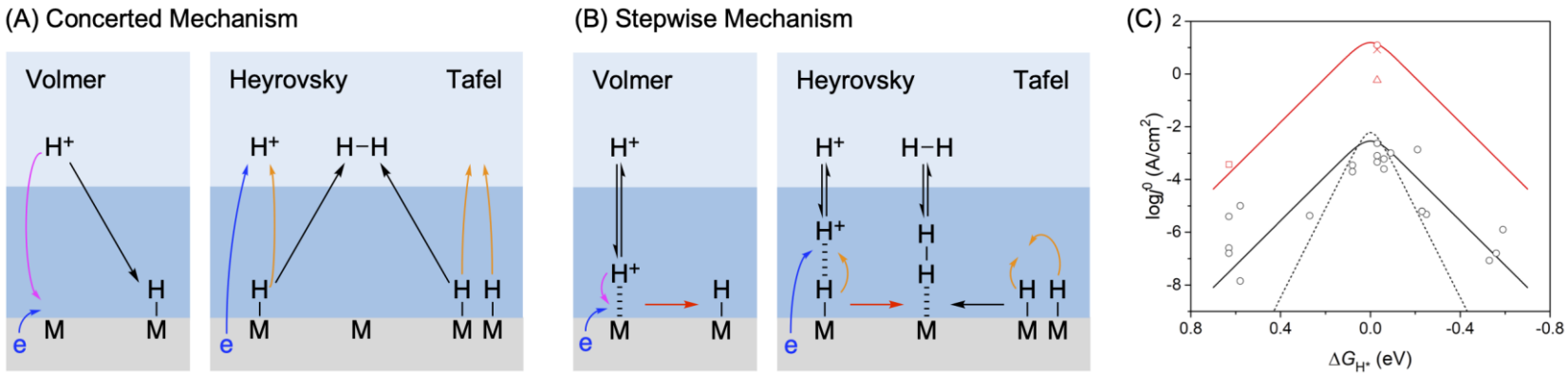

Figure 1. (A) Concerted and (B) stepwise mechanisms of Volmer, Heyrovsky, and Tafel reactions with non-adsorbed and adsorbed species at outer (pale blue) and inner (dark blue) Helmholtz planes, respectively, at the electrode (gray). Blue, purple, and orange arrows indicate the tunneling of electron, proton, and hydrogen, respectively. Red arrows indicate proton-coupled inner-sphere electron transfer. (C) Theoretical (lines) and experimental (symbols) exchange current densities, j^0, against the DFT-based free energy of hydrogen adsorption, ΔG_{H^*} (32). Exchange current densities reported in ref. 32 were calculated from the concerted model (black dashed line) or measured at macroscopic electrodes (black circles). Experimental exchange current densities are also shown for Pt nanoelectrodes (red circle) (7), Pt (red cross) and Au (red square) SECM tips (8), and Pt SECM substrates (red triangle) (9). Red and black solid lines represent the stepwise model, i.e., eq 39 with $f_V + f_H$ = 36 A/cm^2 and 6.6 mA/cm^2, respectively.